

# Experimental Investigation of Acousto-Optic Communications

Lynn Antonelli  
Naval Undersea Warfare Center  
Newport, RI 02841  
[antonelliLT@npt.nuwc.navy.mil](mailto:antonelliLT@npt.nuwc.navy.mil)

Fletcher Blackmon  
Naval Undersea Warfare Center  
Newport, RI 02841  
[blackmonFA@npt.nuwc.navy.mil](mailto:blackmonFA@npt.nuwc.navy.mil)

*Abstract-Covert communications between underwater and aerial platforms would increase the flexibility of surface and air vehicles engaged in undersea warfare by providing a new netcentric warfare communication capability and could have a variety of commercial and oceanographic applications. Research into an acousto-optic sensor shows promise as a means for detecting acoustic data projected towards the water surface from a submerged platform. The laser-based sensor probes the water surface to detect interface vibrations caused by an impinging acoustic pressure field. A number of experimental and simulation studies were conducted to demonstrate acousto-optic sensor feasibility for obtaining robust recordings of acoustic communication signals across the air-water interface. The recorded surface velocity signals were transferred to an acoustic communication receiver that employs conventional acoustic telemetry algorithms such as adaptive equalization and Viterbi convolutional decoding to decode the signal. The detected, equalized, and decoded bit error rate performance is presented for hydrostatic, more realistic hydrodynamic water surface conditions, and hydrodynamic surface conditions while employing a surface normal tracking unit that is designed to mitigate degradation in communication performance as a result of optical signal dropout.*

## I. INTRODUCTION

Traditional sensors to efficiently detect underwater sound must be physically immersed in the water. The air-water boundary constrains communications between underwater and surface or in-air platforms. Typically, remote Radio Frequency (RF) systems are deployed by underwater platforms as a means for communicating with platforms above the water surface. An alternative approach is to exploit the interaction of light and sound at the water surface to obtain information from the sound field in the water. Acousto-optic surface interaction has been studied via several techniques including the detection of phase and/or amplitude modulation of the laser when incident upon a vibrating surface. Interferometric techniques using coherent laser radiation to measure the acoustic signals on a vibrating surface are presented by Belansky and Wasner [1].

The application of a laser Doppler vibrometer (LDV) to measure in-water acoustic signals by probing an air-water, pressure release surface has been more recently

investigated [2-6]. The feasibility tests measured acousto-optic sensitivity values under a range of water surface conditions. Laboratory experiments in support of the laser sensor concept demonstrated reception of tonal and digitized biologic, underwater acoustic signals on the air-water interface. An acoustic source level as low as 120 dB/uPa was detected on the air-water boundary and progress has been made in this sensor research for array beamforming for sound source localization and sensor noise analysis [4,5]. Since successful tests were conducted over a range of discrete tonal frequencies (3 to 50 kHz) and frequency bursts (whale communications signals), it is conceivable that the laser sensor is also capable of detecting composite waveforms such as acoustic communication signals at the water surface.

The reported detection results mark a historical first since there have been no other published studies known to date pertaining to using the laser sensor as an uplink mechanism for underwater communications, that this acousto-optic uplink communication technique is possible [7]. The acousto-optic sensor under hydrostatic conditions demonstrated that data rates of up to 6000 bits per second and higher can be received error free. Under the hydrodynamic conditions reported, data rates of up to 900 bits per second were received error free. It should be noted that the performance degradation under hydrodynamic conditions was dominated by signal dropout at the optical receiver and not by traditional underwater acoustic channel related effects.

$$V = K \cos [2\mathbf{p} (f_0 + 2\mathbf{v} \cdot \mathbf{I})t] \quad (1)$$

The initial test results also provided insight into the various noise mechanisms associated with this sensor technique, specifically with the hydrodynamic condition of the pressure release surface interrogated by the laser system. This acousto-optic uplink communication concept is the counterpart to the current, opto-acoustic transmission research that the authors are conducting in which in-air, high powered, pulsed lasers are being used to transmit acoustic communication signals into the water. Together, the opto-acoustic transmitter and the proposed acousto-optic receiver comprise a bi-directional communications link across the air-water interface [8,9].

A laser-based sensor concept is shown for communicating across the air-water interface. The acousto-optic communication uplink shown in figure 1 outlines a method for detecting acoustic data projected towards the water surface from a submerged platform. The water surface is probed by the laser from the interferometer to

Report Documentation Page				Form Approved OMB No. 0704-0188	
Public reporting burden for the collection of information is estimated to average 1 hour per response, including the time for reviewing instructions, searching existing data sources, gathering and maintaining the data needed, and completing and reviewing the collection of information. Send comments regarding this burden estimate or any other aspect of this collection of information, including suggestions for reducing this burden, to Washington Headquarters Services, Directorate for Information Operations and Reports, 1215 Jefferson Davis Highway, Suite 1204, Arlington VA 22202-4302. Respondents should be aware that notwithstanding any other provision of law, no person shall be subject to a penalty for failing to comply with a collection of information if it does not display a currently valid OMB control number.					
1. REPORT DATE <b>01 SEP 2003</b>		2. REPORT TYPE <b>N/A</b>		3. DATES COVERED <b>-</b>	
4. TITLE AND SUBTITLE <b>Experimental Investigation of Acousto-Optic Communications</b>				5a. CONTRACT NUMBER	
				5b. GRANT NUMBER	
				5c. PROGRAM ELEMENT NUMBER	
6. AUTHOR(S)				5d. PROJECT NUMBER	
				5e. TASK NUMBER	
				5f. WORK UNIT NUMBER	
7. PERFORMING ORGANIZATION NAME(S) AND ADDRESS(ES) <b>Naval Undersea Warfare Center Newport, RI 02841</b>				8. PERFORMING ORGANIZATION REPORT NUMBER	
9. SPONSORING/MONITORING AGENCY NAME(S) AND ADDRESS(ES)				10. SPONSOR/MONITOR'S ACRONYM(S)	
				11. SPONSOR/MONITOR'S REPORT NUMBER(S)	
12. DISTRIBUTION/AVAILABILITY STATEMENT <b>Approved for public release, distribution unlimited</b>					
13. SUPPLEMENTARY NOTES <b>See also ADM002146. Oceans 2003 MTS/IEEE Conference, held in San Diego, California on September 22-26, 2003. U.S. Government or Federal Purpose Rights License, The original document contains color images.</b>					
14. ABSTRACT					
15. SUBJECT TERMS					
16. SECURITY CLASSIFICATION OF:			17. LIMITATION OF ABSTRACT <b>UU</b>	18. NUMBER OF PAGES <b>9</b>	19a. NAME OF RESPONSIBLE PERSON
a. REPORT <b>unclassified</b>	b. ABSTRACT <b>unclassified</b>	c. THIS PAGE <b>unclassified</b>			

detect surface perturbations caused by an impinging acoustic pressure field. The recorded surface velocity signals are transferred to an acoustic communication receiver that uses conventional acoustic telemetry algorithms such as adaptive equalization to decode the signal. Sensor recordings that accurately represent the in-water sound are desired. Signal processing schemes and receiver designs have been successfully used to compensate for phase and amplitude changes of the received acoustic communication signals typically associated with the underwater channel [10-17]. Such algorithms may also be used to compensate for laser sensor phase characteristics potentially leading to improved communications performance. This paper presents the concept of operation of the acousto-optic sensor and the results from a recent feasibility test demonstrating remote communications performance across a dynamic air-water boundary.

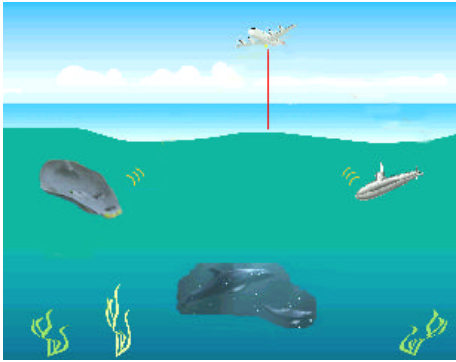


Figure 1. Aerial, Acousto-Optic Communications Conceptualization

## II. PRINCIPLES OF LASER SENSOR OPERATION

The acousto-optic sensor operates by interrogating the air-side of the water surface perpendicularly with low-power, coherent laser radiation from a laser Doppler interferometer. The laser light is focused onto the specularly reflective, air-water boundary to remotely measure the surface velocity. The oscillatory motion of the air-water interface causes the output laser beam of the sensor to travel a slightly longer or shorter distance relative to the nominal surface distance. The effect is a phase (Doppler) shift of the coherent laser radiation, modulated by the oscillations of the water surface due to the in-water acoustic field. The reflected beam, containing the Doppler information, is detected and recombined with the RF modulated reference beam within the interferometer. As a result of heterodyne mixing of the laser beams, an analog voltage signal,  $V$ , containing Doppler information of the normal surface velocity,  $v$ , is then obtained, as indicated in (1).  $K$  is the conversion efficiency constant of the optical

detection,  $f_0$  is the heterodyne frequency shift of the interferometer reference beam,  $\lambda$  is the optical wavelength, and  $t$  is time. The frequency shift of the laser due to the Doppler effect of the surface motion is directly proportional to the surface velocity,  $2v/\lambda$ . The voltage signal from the optical detectors is then filtered and decoded by the LDV electronics where demodulation signal processing is used to extract the velocity information.

## III. SURFACE NORMAL GLINT TRACKING SYSTEM

One solution to the problem of intermittent optical signal dropout as a result of hydrodynamic sea surface conditions is to enlarge the laser beam diameter enough to increase the probability of receiving a reflection from the water surface. Regardless, signal dropout from the hydrodynamic sea surface will not be completely eliminated while incurring a loss in LDV sensitivity. The approach taken in this study to reduce the signal dropout through hardware design was to append a laser-based tracking system to the acousto-optic sensor. The tracking system directs a laser beam in a search pattern on the water surface to find a surface normal such that the reflected laser beam is captured by the system. The tracker then locks on to this surface glint and continually provides a feedback control signal to adjust the mirrors deflecting the beam to maintain position on the surface glint location. The laser beam from the acousto-optic sensor would then be aligned to superimpose on the tracking beam such that it is also continually positioned at the surface reflecting glint location.

The glint tracker system identifies and maintains lock on a water surface reflection feature and continually makes analog corrections to tracking mirrors in real time using a low-power, infrared, incoherent tracking beam. The tracking beam is generated from a laser diode to detect the movements the surface reflectance glint and uses confocal reflectometry to monitor the reflection from the tracking beam's current position. The beam diameter of the tracker system was initially set at approximately 10 mm at the water surface. The laser diode power output was approximately 0.42 mW at a wavelength of 780 nm. The tracker system includes a device for dithering the tracker beam with an oscillatory motion, a tracking device for controlling the position of both the acousto-optic sensor's laser beam and the tracking beam relative to the surface glint, a reflectometer for providing an output signal with a phase corresponding to a phase of the reflected tracking beam, and a signal processor for comparing the phase of the reflectometer output signal to the phases of the oscillatory motion and for controlling the tracking device so that the sensor beam tracks relative to the reference feature [18,19]. The tracker algorithm uses information on

the detected tracker beam amplitude and shape to provide feedback on tracker mirror position to maintain lock on the surface glint.

#### IV. PRINCIPLES OF UNDERWATER ACOUSTIC COMMUNICATION

Current underwater acoustic communication schemes employ either incoherent or coherent signaling techniques. Incoherent techniques are bit or symbol to frequency encoding schemes such as Frequency Shift Keying (FSK) or Multi-Frequency Shift Keying (MFSK). Corresponding receivers rely on Fourier transform techniques to decode the data. Data for these signals has not yet been collected but based on previous tonal studies is considered possible. Instead, the use of coherent signaling techniques is explored.

Coherent techniques are bit or symbol to phase and/or amplitude time domain modulation schemes. This type of signaling provides higher data rate as compared to incoherent signaling techniques for a given bandwidth since the bandwidth efficiency is higher in coherent systems. Typical phase modulation schemes that are used are Binary Phase Shift Keying (BPSK), Quadrature Phase Shift Keying (QPSK), and Trellis Coded Modulated 8-ary Phase Shift Keying (TCM8PSK). A typical amplitude modulation scheme is 16-ary Quadrature Amplitude Modulation (16QAM). Any of these coherent techniques require the use of a joint adaptive decision feedback equalizer (ADFE) and second order Phase Lock Loop (PLL) to compensate for the effect of the underwater channel induced time variation and intersymbol interference inducing multipath structure on the transmitted acoustic signal as seen by the receiver.

Figure 2 shows the general structure of the acoustic telemetry receiver which typically incorporates an equalizer to deal with channel variations, a de-interleaver to randomize residual errors, and a soft decision input decoder which in this case takes the form of a Viterbi decoder to decode the data and correct residual errors. The following figures 3a and 3b show the structures of the equalizer based receiver architectures that were used to process the acoustic communication signals discussed in this paper.



Figure 2. General Acoustic Telemetry Receiver Structure

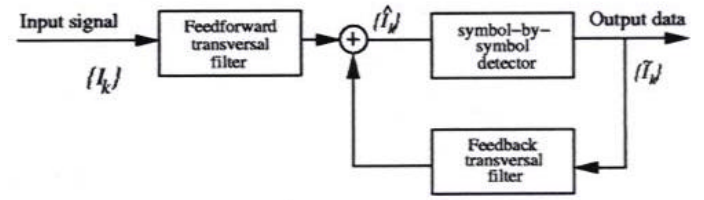


Figure 3a. Normal Decision Feedback Equalizer Structure

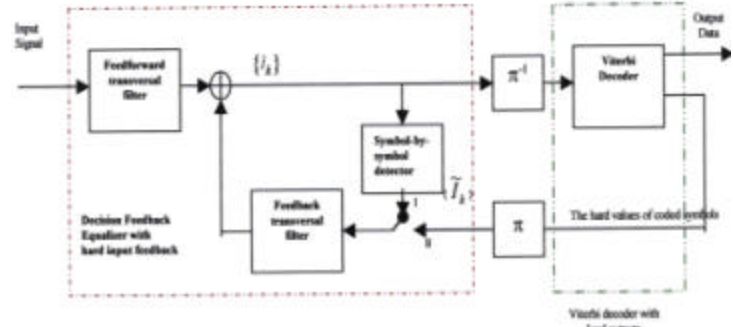


Figure 3b. Hard Iterative Decision Feedback Equalizer Structure

Figure 3a represents the typical equalizer structure for an adaptive DFE that is used in acoustic telemetry applications. Figure 3b represents an improved iterative receiver architecture whereby the decoded, corrected output of the decoder is re-encoded and re-interleaved and passed back to the equalizer as the new training sequence for the entire communication packet instead of training only over a small preamble which is 10% of the total number of packet symbols. At this point, the equalizer processes the data a second time and the decoder is used to decode the data one final time. The objective of using this receiver structure is to obtain as close to the all training condition as possible. It should be noted that more complicated receiver structures with improved performance exist and can be applied in the future if needed [11].

#### V. EXPERIMENT DESCRIPTION

An acoustic communication, water tank test was conducted in which a number of acoustic telemetry signals were transmitted. The signals consisted of BPSK, QPSK, TCM8PSK, and 16QAM modulations with varying degrees of error correction coding, i.e. rate  $\frac{1}{2}$  and rate  $\frac{1}{4}$ . The signal format for each of the signals is shown in figure 4. A BPSK synchronization signal at the beginning of the packet is followed by a time guard band and then followed by coherent modulation which includes a training sequence for the first 10% of the information section of the packet.

A Doppler tone overlaps the entire signal in order to track Doppler variations.

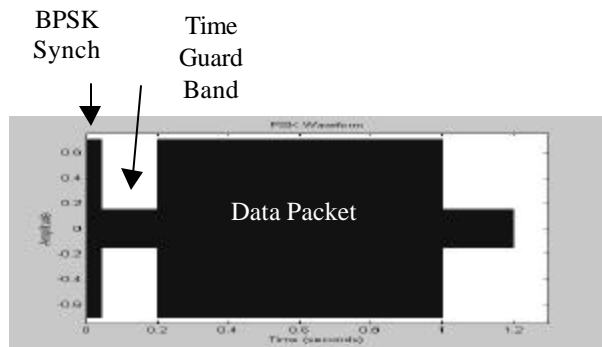


Figure 4. Communication Packet Structure

Experimentation was performed using a single point LDV, (Polytec PI OFV-353) as the acousto-optic sensor to measure the acoustic vibration velocity on the water surface as depicted in figure 5. The surface normal tracker was used to establish acoustic communication performance under hydrodynamic conditions at the Naval Undersea Warfare Center Division Newport's Acoustic Test Facility (ATF). A rotary fan blade was used to create low frequency and low amplitude surface waves. The AN/BQR7 transducer was below the surface and was used to generate acoustic communication waveforms that were received by the laser Doppler vibrometer and surface normal tracker combination. The acousto-optic sensor hardware was positioned at a lateral offset relative to the AN/BQR7 transducer at a distance of approximately 1m above the water surface.

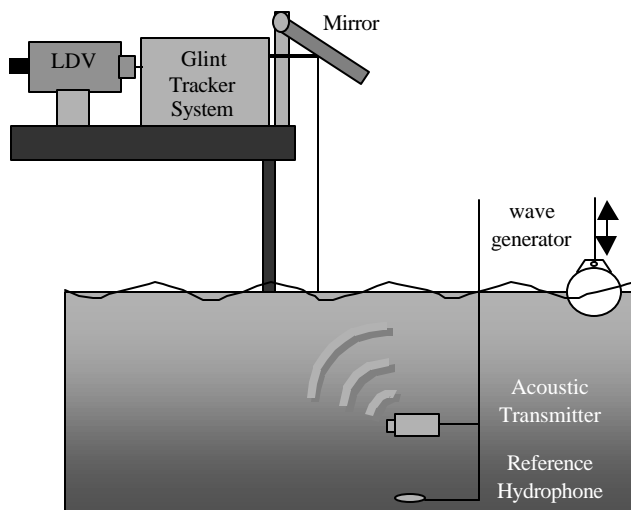


Figure 5. Test configuration for the LDV acousto-optic sensor and the surface normal tracking system.

The data obtained from the test was analyzed to determine acoustic communication performance under hydrodynamic surface conditions with and without the use of the surface normal glint tracking system.

## VI. EXPERIMENTAL RESULTS AND DISCUSSION

Tables I through VIII show the performance obtained using the surface normal tracker under the conditions discussed above. Forty percent of the packets could be synchronized using the synchronization signal that is part of the communication packet structure as shown in Figure 4. Sixty percent of the synchronization signals were not useable due to optical signal loss. It should be noted that without the use of the surface normal tracker few if any packets could be synchronized and decoded properly. The equalizer performance is tabulated for the receiver in Fig 3a. The number of symbols lost due to loss of optical return into the acousto-optic sensor and the percent symbol loss is indicated. The performance of the equalizer under the all training condition, which is the potential optimum performance of the receiver in figure 3b, is also shown. The BPSK results for  $\frac{1}{2}$  rate constraint length 9 convolutional code for the case of no diversity and time diversity are shown respectively in tables I and II. The BPSK results for  $\frac{1}{4}$  rate constraint length 9 convolutional code for the case of no diversity and time diversity are shown respectively in tables III and IV. The QPSK results for  $\frac{1}{2}$  rate constraint length 9 convolutional code for the case of no diversity and time diversity are shown respectively in tables V and VI. The QPSK results for  $\frac{1}{4}$  rate constraint length 9 convolutional code for the case of no diversity and time diversity are shown respectively in tables VII and VIII. The data rate in each case after decoding is listed. The clipping threshold during the data demodulation stage prior to equalization was set to 0.01 for the BPSK signals and set to 0.008 for the QPSK signals. Values above the threshold are set to zero in the demodulated data to account for the clipped signal sections as a result of data dropout due to optical signal loss at the acousto-optic sensor. The equalizer settings that were used to process the data were  $L=5$  feedforward filter symbols,  $M=5$  feedback filter symbols, forgetting factor = 0.995, and phase tracking constants  $K1=0.001$  and  $K2=0.0001$ .

In the BPSK no diversity case, the bit error rate (BER) was 2.7% and 4.7% respectively for the  $\frac{1}{2}$  rate and  $\frac{1}{4}$  rate coded cases. There was one case where the number of errors is excessive, 463. This represents a 25% error within this packet. The high number of errors was due to the condition of signal dropout while the equalizer was trying to train to the channel. Using iteration, the error for this packet can be reduced such that the decoder can produce near errorless results. In all other cases, the BER was low enough at the output of the equalizer that the

decoder following the de-interleaving process could decode each packet to produce no errors.

In the BPSK time diversity case, the BER was 0.18% and 1.6% respectively for the  $\frac{1}{2}$  rate and  $\frac{1}{4}$  rate coded cases. Use of time diversity eliminates the high error packet condition encountered in the no diversity case. The BER was low enough at the output of the equalizer, significantly better than the no diversity case, that the decoder following the de-interleaving process could decode each packet to produce no errors.

In the QPSK no diversity case, the bit error rate (BER) was 8.9% and 7.9% respectively for the  $\frac{1}{2}$  rate and  $\frac{1}{4}$  rate coded cases. There are four cases where the number of errors was excessive, the error percentage on a packet basis was between 14% and 51%. The number of errors in these cases may be substantially lowered to approximately 10% BER per packet by either lowering the clipping threshold to 0.004 or by using phase tracking constants of  $K1=0.005$  and  $K2=0.0005$ . The high number of errors was due to the condition of signal dropout occurring within isolated clusters within the data packet. In all other cases, the BER was low enough at the output of the equalizer that the decoder following the de-interleaving process could decode each packet to produce no errors. The BER in the all training situation was respectively 2.4% and 1.8%, demonstrating the performance improvement that could be obtained by varying degrees of iterative processing.

In the QPSK time diversity case, the BER was 4.8% and 1.8% respectively for the  $\frac{1}{2}$  rate and  $\frac{1}{4}$  rate coded cases. Use of time diversity eliminates all but one of the high error packet conditions encountered in the no diversity case. The BER was low enough at the output of the equalizer, significantly better than the no diversity case, that the decoder following the de-interleaving process could decode every packet except the first entry in table VI to produce no errors.

The BER in the all training situation was respectively 0.47% and 0.24%, demonstrating the performance improvement that could be obtained by varying degrees of iterative processing.

## VII. CONCLUSIONS

The surface normal tracker in conjunction with the laser Doppler vibrometer provided the capability for the acousto-optic sensor to function in low amplitude and low frequency hydrodynamic air-water boundary conditions at sensor to water surface distances that would not be possible with only the laser Doppler vibrometer. Without the surface normal tracker in operation, degradation in communication performance as a result of optical signal dropout precluded synchronization and equalization of the data. This result, therefore, demonstrates the need for the surface normal tracking system. The equalizer

performance using the surface normal tracker has been demonstrated for BPSK and QPSK coherent signals.

Robust performance providing errorless performance has been demonstrated for almost all of the packets that could be synchronized. However, it should be noted that the test geometry was fixed and the remaining packets that have a compromised synchronization signal could be processed based on a running history of synchronization points. In practice though, the Doppler may not be known and therefore synchronization must be established on a packet by packet basis. An important aspect of the surface normal tracking system that has not been explored in this paper is the added burden that the changing sensing point, i.e. complex trajectory of the laser sensing beam on the air-water boundary has on the equalizer's tracking capability. No explicit compensation within the equalizer has been attempted thus far to deal with the impact on the phase estimates, Doppler estimates, and adaptive filter weight updates.

## VIII. FUTURE RESEARCH

Future research areas relate to the improvement and application of the communications link. The design and use of more sensitive, optimal light collecting interferometric sensors would improve communication performance as well as general sensing performance. The authors are currently involved in pursuing and improving a surface normal tracking capability that would insure that light is collected at all times by the sensor by tracking the water surface normal to the incident laser interrogation beam while in real time directing the interrogation beam to that position on the water surface in order to receive the optical returns. This system improvement would lower the signal dropout percentage for each communication packet, which appears to be one of the limiting factors for the use of the acousto-optic sensor. Spatial diversity combining of optical returns would improve the performance of the overall system by applying multiple sensors to receive the communication signals that could be jointly, coherently equalized. More complicated receiver architectures that employ alternate equalizer and decoder structures with multiple iteration or integral processing capability can improve communication performance as well.

It is of interest to combine this acousto-optic communication uplink with an opto-acoustic communication downlink that the authors are currently pursuing. Each of these data links and capabilities that they afford are being explored to support a broad range of commercial and military applications that serve as a comprehensive basis for future research.

## IX. REFERENCES

- [1] Belansky, R.H., and Wanser, K.H., "Laser Doppler velocimetry using a bulk optic Michelson interferometer: A student laboratory experiment", *American Journal of Physics* 61(11):1014-1019, November 1993.
- [2] Antonelli, L. and Walsh K., "Photon Transducer", US Patent 6,188,644, February 2001.
- [3] Antonelli, L., Walsh K. and Alberg, A., "Laser interrogation of the air-water interface for in-water sound detection: Initial feasibility tests," 138<sup>th</sup> Meeting of the Acoustical Society of America (ASA), Columbus, Ohio, 3-5 November 1999.
- [4] Antonelli, L., Kirsteins, I., "Bearing estimation error analysis using laser acoustic sensor measurements on a hydrodynamic surface," *Proceedings of the Oceans 2000 Conference*, p.999-1004, September 2000.
- [5] Antonelli, L., Kisteins, I., "Empirical Acousto-Optic Sonar Performance Versus Water Surface Conditions," *Proceedings of the Oceans 2001 Conference*, p.?-?, November 2001.
- [6] Matthews, A. and Arrieta, L., "Acoustic optic hybrid (AOH) sensor," *J. Acoustical Society of America*, 108(3) Pt. 1:1089-1093, September, 2000.
- [7] Blackmon, F., Antonelli, L., Estes, L., and Fain, Gilbert, "Experimental investigation of underwater to in-air communications," *Proceedings of the Undersea Defense Technology (UDT) Europe Conference*, LaSpezia, Italy, June 2002.
- [8] Blackmon, F., "Linear and Non-Linear Opto-Acoustic Communications", Naval Undersea Warfare Center, Division, Newport, RI, TM#990108.
- [9] Blackmon, F., "Linear Opto-Acoustic Communications", Naval Undersea Warfare Center, Division Newport, RI, TM#980144.
- [10] Stojanovic, M., "Recent Advances in High-Speed Underwater Acoustic Communications," *IEEE Journal of Oceanic Engineering*, 21(2):125-136, April, 1996.
- [11] Blackmon, F., Sozer, E., Hagh, M., Proakis, J., and Salehi, M., "Performance Comparison of Iterative/Integral Equalizer/Decoder Structures for Underwater Acoustic Channels," *Proceedings of the Oceans 2001 Conference*, November 2001.
- [12] Blackmon, F. and Canto, W., "Performance Comparison of Several Contemporary Equalizer Structures Applied to Selected Field Test Data," *Proceedings of the Oceans 2000 Conference*, September, 2000.
- [13] Blackmon, F., Jarvis, S., Morrissey, R., Lambert, D., "High-Rate Underwater Acoustic Telemetry with Naval Applications", *Sea Technology*, Vol. 40, May 1999.
- [14] Jarvis, S. and Blackmon, F. "An Acoustic Telemetry System for Use on Undersea Ranges", *JASA*, Vol. 102, November 1997.
- [15] Blackmon, F., "Error-Rate Performance of Convolutionally Encoded. Interleaved QPSK and 8PSK TCM Underwater Acoustic Telemetry", *JASA* Vol. 102, November 1997.
- [16] Jarvis, S., Blackmon, F., Fitzpatrick, K., Morrissey, R., "Results of Recent Sea Trials of the Underwater Digital Acoustic Telemetry System", *Proceedings of the Oceans 1997 Conference*, October, 1997.
- [17] Carvalho, D., Blackmon, F., Janiesch, R., "The Results of Several Acoustic Telemetry Tests in Both Shallow and Deep Water", *Proceedings of the Oceans 1995 Conference*, October 1995.
- [18] Ferguson, D., "Servo tracking system utilizing phase-sensitive detection of reflectance variations," U.S. Patent number 5,767,941, June 16, 1998.
- [19] Ferguson, D., "Servo tracking system utilizing phase-sensitive detection of reflectance variations," U.S. Patent number 5,943,115, August 24, 1999.

Table I. BPSKHALFRAND (No Diversity) (data rate after decode = 900 bits/sec)

File #	# Symbols Lost	% Symbols Lost	Equalization Method	# Equalizer Errors
0	43	2.2	Normal	37
1	55	2.8	Normal	73
2	57	2.9	Normal	56
3	32	1.6	Normal	32
4	39	2.0	Normal	40
5	88	4.4	Normal	81
6	12	0.6	Normal	20
7	73	3.7	Normal	66
8	38	1.9	Normal	22
9	40	2.0	Normal	53
BER				2.7%

Note: clipping threshold set to 0.01. L=5, M=5, lambda=0.995, K1=0.001, K2=0.0001

Table II. BPSKHALFRAND (Time Diversity) (data rate after decode = 450 bits/sec)

File #	Equalization Method	# Equalizer Errors
0,1	Normal	41
2,3	Normal	29
4,5	Normal	17
6,7	Normal	10
8,9	Normal	19
BER		1.3%

Note: clipping threshold set to 0.01. L=5, M=5, lambda=0.995, K1=0.001, K2=0.0001

Table III. BPSKQUARRAND (No Diversity) (data rate after decode = 450 bits/sec)

File #	# Symbols Lost	% Symbols Lost	Equalization Method	# Equalizer Errors
0	33	1.7	Normal	39
1	14	0.7	Normal	25
2	81	4.1	Normal	78
3	33	1.7	Normal	39
4	29	1.5	Normal	26
5	64	3.2	Normal	48
6	75	3.8	Normal	92
7	63	3.2	Normal	463*
8	10	0.5	Normal	19
9	17	0.9	Normal	22
BER				4.7%

Note: clipping threshold set to 0.01. L=5, M=5, lambda=0.995, K1=0.001, K2=0.0001

\* = clipped during training



Table IV. BPSKQUARRAND (Time Diversity) (data rate = 225 bits/sec)

File #	Equalization Method	# Equalizer Errors
0,1	Normal	18
2,3	Normal	39
4,5	Normal	16
6,7	Normal	59
8,9	Normal	12
BER		1.6%

Note: clipping threshold set to 0.01. L=5, M=5, lambda=0.995, K1=0.001, K2=0.0001

Table V. QPSKHALFRAND (No Diversity) (data rate after decode = 1800 bits/sec)

File #	# Symbols Lost	% Symbols Lost	Equalization Method	# Equalizer Errors	# Equalizer Errors (All Train)
0	142	7.1	Normal	502*	225
1	39	2	Normal	610*	61
2	71	3.6	Normal	140	70
3	123	6.2	Normal	1450*	201
4	77	3.9	Normal	171	99
5	73	3.7	Normal	188	120
6	0	0	Normal	0	0
7	62	3.1	Normal	156	84
8	0	0	Normal	0	0
9	0	0	Normal	0	0
BER				8.9%	2.4%

Note: clipping threshold set to 0.008. L=5, M=5, lambda=0.995, K1=0.001, K2=0.0001

\* = somewhat better performance obtained when K1=0.005, K2=0.0005

\* = somewhat better performance obtained when clipping threshold set to 0.004

Table VI. QPSKHALFRAND (Time Diversity) (data rate after decode = 900 bits/sec)

File #	Equalization Method	# Equalizer Errors	# Equalizer Errors (All Train)
0,1	Normal	543*	26
2,3	Normal	131	26
4,5	Normal	174	33
6,7	Normal	14	0
8,9	Normal	0	0
BER		4.8%	0.47%

Note: clipping threshold set to 0.01. L=5, M=5, lambda=0.995, K1=0.001, K2=0.0001

\* = somewhat better performance obtained when K1=0.005, K2=0.0005

\* = somewhat better performance obtained when clipping threshold set to 0.004

Table VII. QPSKQUARRAND (No Diversity) (data rate after decode = 900 bits/sec)

File #	# Symbols Lost	% Symbols Lost	Equalization Method	# Equalizer Errors	# Equalizer Errors (All Train)
0	31	1.6	Normal	65	36
1	34	1.7	Normal	57	37
2	82	4.1	Normal	216	115
3	79	4.0	Normal	171	82
4	26	1.3	Normal	82	50
5	55	2.8	Normal	175	111
6	61	3.1	Normal	1851*	117*
7	8	0.4	Normal	36	16
8	28	1.4	Normal	66	36
9	43	2.2	Normal	107	51
BER				7.9%	1.8%

Note: clipping threshold set to 0.008. L=5, M=5, lambda=0.995, K1=0.001, K2=0.0001

\* = somewhat better performance obtained when K1=0.005, K2=0.0005

\* = somewhat better performance obtained when clipping threshold set to 0.004

Table VIII. QPSKQUARRAND (Time Diversity) (data rate after decode = 450 bits/sec)

File #	Equalization Method	# Equalizer Errors	# Equalizer Errors (All Train)
0,1	Normal	7	1
2,3	Normal	147*	11
4,5	Normal	70	11
6,7	Normal	50	11
8,9	Normal	53	9
BER		1.8%	0.24%

Note: clipping threshold set to 0.01. L=5, M=5, lambda=0.995, K1=0.001, K2=0.0001

\* = somewhat better performance obtained when K1=0.005, K2=0.0005

\* = somewhat better performance obtained when clipping threshold set to 0.004